

## Emission and Friction Analysis of IC Engine Running in Methanol Blend

A. Gupta<sup>a</sup>, P.C. Mishra<sup>a</sup>

<sup>a</sup>Green Engine Technology Center, School of Mechanical Engineering, KIIT University Bhubaneswar, India.

### Keywords:

Emission  
Friction  
Tribology  
Condition monitoring

### ABSTRACT

Emission and friction are considered to be the significant contributors towards engine parasitic losses. Inherent engine design responsible for such irregularities is difficult to eliminate totally, as millions of engines operating in such principle cannot be replaced. Therefore, only partial modification is allowed to achieve slight improvement in fuel economy and performance improvement. Such improvement is possible through condition monitoring of IC engine through emission and friction analysis. Using an emission analyzer, the emission gases such as CO, CO<sub>2</sub>, NO<sub>x</sub>, HC, lambda (air fuel ratio) are monitored for three different petrol and methanol blend (M5, M10, M15). The brake power response to rpm for different torque and speed are monitored from the engine coupled with eddy current dynamo meter and mounted in a universal engine test bed. Friction power loss is numerically estimated through tribological principles and validated with experimental results.

### Corresponding author:

Prakash Chandra Mishra  
Green Engine Technology Center,  
School of Mechanical Engineering,  
KIIT University,  
Patia, Bhubaneswar, India.  
E-mail: pmishrafme@kiit.ac.in

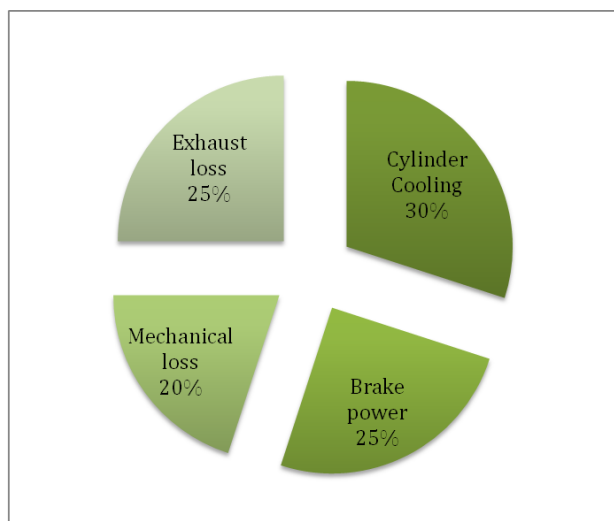
© 2018 Published by Faculty of Engineering

## 1. INTRODUCTION

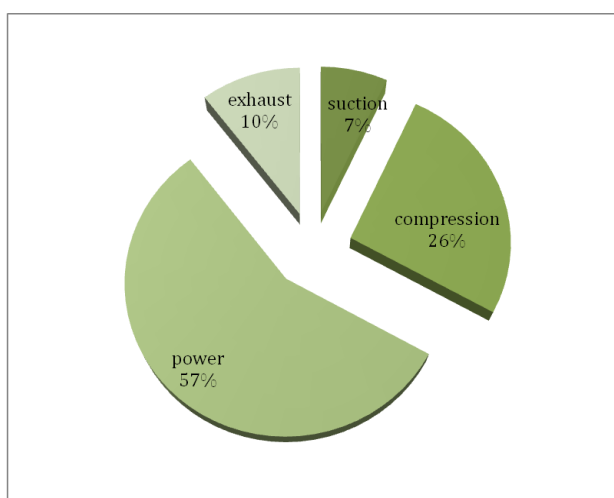
Emission and friction accounts more than 45 % of the total input fuel energy [1]. It is because of inherent engine design, based on which millions of vehicles running on the road. For economic prospective it is not possible to total replacement of the propulsion system of vehicle. Partial modification to improve engine performance through reduction of emission and friction can help save the fuel and enhance life.

Emission is a thermodynamic phenomena, while friction is a phenomena related to dynamic engine components on contact. Further, understanding emission requires the knowledge of the primary components of emission: CO, CO<sub>2</sub>,

NO<sub>x</sub>, HC, O<sub>2</sub>, which has the undesired effect on environment and also on the engine efficiency and performance [2]. The parameters controlling such constituents of exhaust are the engine speed, torque, brake specific fuel consumption, air fuel ratio, throttle etc. [3]. In order to minimize these harmful emissions, many attempts are made [4-6]. Among them 'use of alternate fuel' is one effective step in this direction. Instead of petrol/diesel, the blend of bio fuels with either of them is found to be useful exercise, that helps in reducing the greenhouse gases to significant extent. Alcoholic blends are most useful in preparing alternate fuels without affecting the toxicity and acid value. Methanol, Ethanol, Propanol and Butanol are most widely used alcoholic blends in petrol and diesel respectively.



(a)



(b)

**Fig. 1.** (a) Engine losses and (b) friction losses [3].

From the literature, it is found out that though there is appreciable reduction in carbon related emissions due to use of alternate blended fuels, there is elevated emission of  $\text{NO}_x$  due to such fuel modification [7]. It is found that because of better combustion, the exhaust temperature of the engine increases which leads to the enhancement of  $\text{NO}_x$ .  $\text{NO}_x$  also has harmful effect on environment. It can be controlled through various methods such as 'use of catalytic converter' [8], design modification of muffler [9], 'enhancement of surface area' etc.

Friction arises in IC engine is due to many relatively moving parts in contact [10-12]. That includes ring-liner, skirt-liner, ring-ring groove, cam-follower etc. to name few. Among the same, piston subsystem friction losses are major losses accounts more than 80 % of total parasitic losses [13]. The piston subsystem components are

designed for simultaneous sealing and easy sliding. Chronological development of the same every time ensures better sealing and easy sliding characteristics. Such conjunctions are mostly lubricated and dried some times while in engine running. The thermo hydrodynamic analysis [14] helps solving for the friction force/power by solving coupled Reynolds and Energy equation [15]. Because of regime transition, there is need of solving Reynolds equation for hydrodynamic, mixed in separate form. In the vicinity of dead centers [10]. Operational parameters like sliding velocity, external loads; lubricant rheological properties like viscosity, density, pressure, temperature; conjunction geometry such as contact surface roughness, asperity tip radius, asperity density play important role in controlling frictional characteristics. Through these parameters, hydrodynamic/EHL pressure, friction (boundary, mixed or hydrodynamic) force/power can be monitored. To improve existing design, it is essential to monitor such parameters.

Though there are number of research work carried out to reduce emission constituents like  $\text{CO}$ ,  $\text{CO}_2$ , and  $\text{HC}$  etc by the use of alternate fuel [17-19] and friction analysis, condition monitoring of engine through emission and friction analysis will be a step further in this research.

## 2. EXPERIMENTAL METHOD FOR EMISSION MONITORING

### 2.1 Characterization of Petro and Methanol blend

The Methanol is abundantly available alcoholic member, which because of its light weight, mixed better with petrol and subject to better combustion. In the current analysis, three different blends are tested for emission and performance. These are M5 (95 % petrol and 5 % Methanol), M10 (90 % petrol and 10% Methanol) and M15 (85 % petrol and 15% Methanol). The Table 1 represents the characterization of the hand blended alcoholic mixture.

The emission monitoring procedure includes mounting the four stroke single cylinder engine in the universal engine test bed and coupling the same to the Eddy current dynamometer with data acquisition system. The dynamo is capable

of testing engine with 90 Nm torque. The speed of the engine is to be controlled through required throttling.

**Table 1.** Characterization of blended fuel.

Fuel properties	Standard testing protocol	Pure petrol	M5	M10	M15
Density (kg/L)	ASTM 4052	0.745	0.742	0.736	0.732
Kinematic viscosity (C Stoke)	ASTM D445	0.88	0.86	0.84	0.81
Acid value (mg KOH/g)	ASTM D664	0.32	0.30	0.295	0.29
Flash point (0C)	ASTM D93	246	244	242	241
Calorific value (kJ/kg)	ASTM D240	47300	47230	47129	46965



(a)



(b)



(c)



(d)

**Fig. 2.** Experimental arrangement for emission analysis: (A) Blending of fuel, (B) Eddy current data acquisition, (C) Emission analyzer and (D) Emission sensing.

The engine with the specifications mentioned in Table 2 is subjected to run in different pair of torque and rpm. The emission details are sensed using a six gas emission analyzer. At the steady state of the engine the components of emission: CO, CO<sub>2</sub>, NO<sub>x</sub>, HC, O<sub>2</sub> are recorded in a transition of 120 seconds. The analyzer stored the data at every 3 seconds in excel format.

**Table 2.** Engine Specification [3].

Engine parameters	Detail
Engine type	Air-cooled, 4-stroke, SOHC, 2-valve
Cylinder arrangement	Single-cylinder
Cylinder displacement	105.6 cc
Bore & Stroke	49.0 x 56.0 mm
Compression ratio	9.0:1
Maximum power	7.6PS (5.59 kW) / 7,500 rpm
Maximum torque	7.85N.m / 6,000 rpm
Lubrication	Wet sump
Carburetion	Mikuni VM17SS
Ignition system	C.D.I
Primary / Secondary reduction ratio	3.722 / 3.143
Clutch type	Wet multi-plate coil spring
Transmission type	Four speed constant mesh
Gear ratio	3.00, 1.688, 1.2 and 0.875 respectively for 1st, 2nd, 3rd and 4th respectively
Engine oil capacity	1 liter

The operating procedure of HORIBA MEXA-584L emission analyzer includes the calibration of the analyzer at the first time use with help of gas canisters with leveled concentration. Before using the analyzer for emission analysis, the leak proof test is done. Later, it is necessary to carry out HC hangup test and then the analyzer is ready to measure the emissions. Now the engine

is manually started. The gear is set to achieve required torque and rpm.

The dyno control panel is equipped with control system, which can monitor the brake power response to speed. The reading can be taken for constant torque or constant rpm. Along with the load, speed, brake power, the panel has provisions to measure, exhaust gas temperature, oil temperature, gas pressure etc. through thermo-couple and pressure gauges. The braking torque offered by dynamometer is sensed through NI's load shell fitted on the base of the dynamometer.

### 3. NUMERICAL METHOD FOR FRICTION MONITORING

Ring-liner contact is most friction contributing pair in engine due to simultaneous sealing and sliding action. Hence, it is required to understand friction mechanism through mathematical modeling. The numerical methods of friction monitoring involve the formulation of appropriate equation for ring-liner contact.

#### 3.1 Theory of ring-liner friction

It is difficult to monitor the frictional behavior of a running engine experimentally. Only the brake power can be monitored, which gives gross idea on friction issue. In other ways, the use numerical methods if developed can predict the details of tribological issues of running engine. It gives virtual reality of detailed friction performance.

The friction energy loss is mathematically given as:

$$\Sigma P_f = \Sigma Fv \quad (1)$$

where:

$$F = \iint \tau dx dy \quad (2)$$

and  $v$  = the piston sliding velocity (m/s).

The shear stress of the lubricant can be found out from equation (3).

$$\tau = \frac{\eta U}{h} (\phi_{fs} + \phi_{fs}) - \phi_{fp} \frac{h}{2} \frac{\partial p}{\partial x} \quad (3)$$

Here, the hydrodynamic pressure developed is responsible to separate the two relatively

moving parts. As the friction is significant during the mixed regime of lubrication [16], it is obtained by solving flow averaged Reynolds equation as given in equation (4).

$$\frac{\partial}{\partial x} \left( \phi_x \frac{h^3}{12\eta} \frac{\partial p_h}{\partial x} \right) + \frac{\partial}{\partial y} \left( \phi_y \frac{h^3}{12\eta} \frac{\partial p_h}{\partial y} \right) = \frac{U_1 + U_2}{2} \frac{\partial (\phi_s h)}{\partial x} + \frac{U_1 - U_2}{2} \sigma \frac{\partial \phi_s}{\partial x} + \frac{\partial h}{\partial t} \quad (4)$$

The momentary cessation at the dead centers resulted the sliding velocity to be zero and the Reynolds equation failed to predict the pressure, if there is insufficient squeeze film action. The friction details can be in this case predicted through consideration of boundary phenomena. The asperity contact pressure [16] is one of the important parameter given through equation (5).

$$P_{asp} = K^* E' F_{2.5}(\lambda) \quad (5)$$

where:

$$K^* = 5.318748 \times 10^{10} \beta_{rk}^{5/2} \quad (6)$$

$$E' = \frac{1}{\left( \frac{1 - \nu_1^2}{E_1} + \frac{1 - \nu_2^2}{E_2} \right)} \quad (7)$$

and:

$$F_{2.5}(\lambda_{rk}) = \frac{1}{\sqrt{2\pi}} \int_{\lambda_{rk}}^{\infty} (s - \lambda_{rk})^{5/2} e^{-s^2} ds \quad (8)$$

$F_{2.5}(\lambda_{rk})$  is obtained through non-linear approx. of Gaussian value to linear equation [10].

The friction mean effective pressure which is an important parameter is helpful in comparing different engine performance is given in equation (9).

$$P_{mep} = \frac{2P_c(k)}{N.V_d(k)} \quad (9)$$

where:  $P_c(k)$  is the power at  $k^{\text{th}}$  crank angle,  $V_d(k)$  is the displacement volume in cubic meter and  $N$  is the engine speed in revolution per second. The viscosity temperature inters dependency affect the friction behavior at lot. In engine operating environment, the temperature is obviously in higher order, further sliding action and lubrication shear added additional 90 °C. The viscosity-temperature relation is given as in equation (11).

$$\eta = \eta_s e^{\alpha p - \beta \theta} \quad (10)$$

### 3.2 Computational steps and boundary conditions

The computational steps for this numerical formulation involve quantifying the film shape through geometry approximation. Then, discretisations of Reynolds equation for pressure and energy equation for temperature are formulated. Further to this analysis, initiation of grid of (180x200) in the unwrapped contact surface initialization of temperature and pressure. Computation of further values using an iterative algorithm of effective influence Newton Raphson method to converge the temperature and pressure error. Finally, estimation of fluid shear, friction force (through areal integration), friction power (multiplying sliding velocity to the friction at each crank location. Then frictional energy per cycle is the summation the powers in of all crank angle. The model thus developed follows the validation process as discussed in [15].

### 4. RESULT AND DISCUSSIONS

The emission measured for different torque and speed conditions are given in the Tables 3-11. The torque is set to 5 Nm. The results show that CO concentration of the exhaust decrease with increasing engine speed from 500-1500 rpm. The highest being 7.09 (% vol) at 500 rpm during 20<sup>th</sup> second of measurement. All the measurements are taken for the M5, M10 and M15 blended fuel. Change of rpm have little effect on CO<sub>2</sub> emission from an engine. The next major emission constituent is NO<sub>x</sub>. Its impact on environment is hazardous. Though the carbon-emission components reduced due to alternate/blended fuel use, the NO<sub>x</sub> is enhanced. From the Tables 3-5, the NO<sub>x</sub> increases with increasing rpm, as the exhaust temperature increases. The highest NO<sub>x</sub> recorded at 120<sup>th</sup> second at 1500 rpm.

**Table 3.** Emission constituents at 5 Nm and 500 rpm, M5.

Pass time (s)	CO (% V)	CO <sub>2</sub> (% V)	NO <sub>x</sub> (ppm V)	HC (ppm V)	O <sub>2</sub> (%V)
0	2.56	2.84	102	61	14.5
20	2.59	2.8	106	64	14.5
40	2.83	2.8	106	63	14.35
60	2.63	2.74	102	60	14.55
80	2.69	2.8	111	64	14.5
100	2.55	2.72	108	60	14.6
120	2.86	3.00	111	58	14.21

**Table 4.** Emission constituents at 5 Nm and 500 rpm, M10.

Pass time (s)	CO (% V)	CO <sub>2</sub> (% V)	NO <sub>x</sub> (ppm V)	HC (ppm V)	O <sub>2</sub> (%V)
0	6.42	2.08	121	209	13.86
20	7.22	2.32	122	235	13.5
40	6.31	2.18	122	203	13.95
60	6.32	2.1	117	213	14
80	6.9	2.2	120	200	13.5
100	6.63	2.12	115	201	13.8
120	6.26	2.2	116	194	13.9

**Table 5.** Emission constituents at 5 Nm and 500 rpm, M15.

Pass time (s)	CO (% V)	CO <sub>2</sub> (% V)	NO <sub>x</sub> (ppm V)	HC (ppm V)	O <sub>2</sub> (%V)
0	6.42	4.66	135	82	10.69
20	7.09	4.96	149	72	10.51
40	6.31	5.08	147	62	10.64
60	6.32	5.14	147	48	10.71
80	6.9	5.24	145	39	10.8
100	6.63	5.28	142	33	10.89
120	6.63	5.3	140	29	11.03

**Table 6.** Emission constituents at 5 Nm and 1000 rpm, M5.

Pass time (s)	CO (% V)	CO <sub>2</sub> (% V)	NO <sub>x</sub> (ppm V)	HC (ppm V)	O <sub>2</sub> (%V)
0	3.15	3.5	181	88	13.4
20	2.65	3.16	182	84	14.1
40	3.00	3.8	195	81	13.4
60	3.08	3.58	195	84	13.3
80	2.89	3.56	203	84	13.5
100	2.97	3.64	207	79	13.3
120	2.87	3.52	209	73	13.5

**Table 7.** Emission constituents at 5 Nm and 1000 rpm, M10.

Pass time (s)	CO (% V)	CO <sub>2</sub> (% V)	NO <sub>x</sub> (ppm V)	HC (ppm V)	O <sub>2</sub> (%V)
0	2.59	3.38	139	69	13.8
20	2.4	3.4	136	64	13.7
40	2.43	3.34	136	66	13.8
60	2.34	3.38	143	61	13.8
80	2.4	3.42	146	57	13.7
100	2.22	3.2	141	58	14.2
120	2.56	3.48	155	55	13.7

**Table 8.** Emission constituents at 5 Nm and 1000 rpm, M15.

Pass time (s)	CO (% V)	CO <sub>2</sub> (% V)	NO <sub>x</sub> (ppm V)	HC (ppm V)	O <sub>2</sub> (%V)
0	2.74	4.26	185	63	12.6
20	3.55	4.24	199	62	12.64
40	2.47	4.26	205	58	12.61

60	2.38	4.31	210	55	12.67
80	2.35	4.36	219	52	12.61
100	2.29	4.52	237	51	12.2
120	2.01	4.30	250	48	12.63

**Table 9.** Emission constituents at 5 Nm and 1500 rpm, M5.

Pass time (s)	CO (% V)	CO <sub>2</sub> (% V)	NO <sub>x</sub> (ppm V)	HC (ppm V)	O <sub>2</sub> (%V)
0	5.35	4.7	270	89	10.8
20	4.93	4.62	276	87	11.1
40	4.71	4.66	284	84	11.1
60	3.86	4.44	267	71	11.67
80	4.89	4.66	283	88	11.1
100	4.66	4.7	285	84	11.1
120	3.46	4.66	283	88	11.1

**Table 10.** Emission constituents at 5 Nm and 1500 rpm, M10.

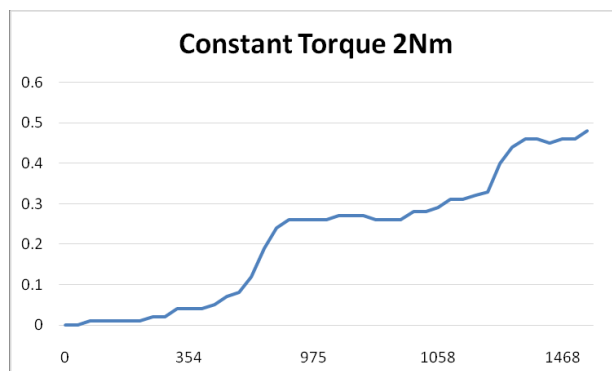
Pass time (s)	CO (% V)	CO <sub>2</sub> (% V)	NO <sub>x</sub> (ppm V)	HC (ppm V)	O <sub>2</sub> (%V)
0	3.46	4.1	222	64	12.6
20	3.25	4.02	220	62	12.6
40	4.71	4.1	230	62	12.5
60	3.3	4.1	230	62	12.5
80	3.27	4.02	234	62	12.4
100	3.44	4.16	253	67	12.3
120	3.88	4.16	244	66	12.3

**Table 11.** Emission constituents at 5 Nm and 1500 rpm, M15.

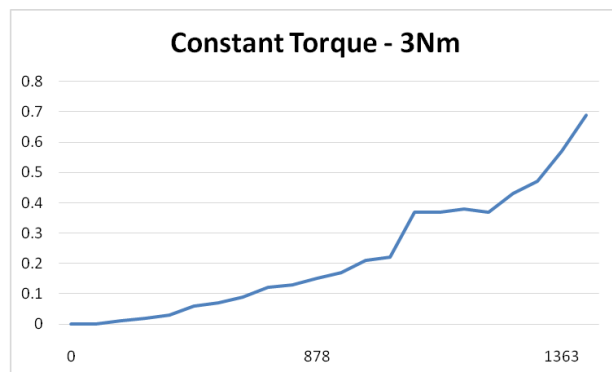
Pass time (s)	CO (% V)	CO <sub>2</sub> (% V)	NO <sub>x</sub> (ppm V)	HC (ppm V)	O <sub>2</sub> (%V)
0	3.95	4.96	315	80	11.09
20	2.55	4.86	308	82	11.27
40	2.47	4.82	318	81	11.24
60	2.38	4.82	320	80	11.28
80	2.35	4.86	325	81	11.2
100	2.29	4.92	364	82	11.12
120	2.01	4.9	339	83	11.16

The un-burnt HC has found no effect within the time of monitoring in 1500 rpm. Also O<sub>2</sub> concentration has also not been effected due to the pass time.

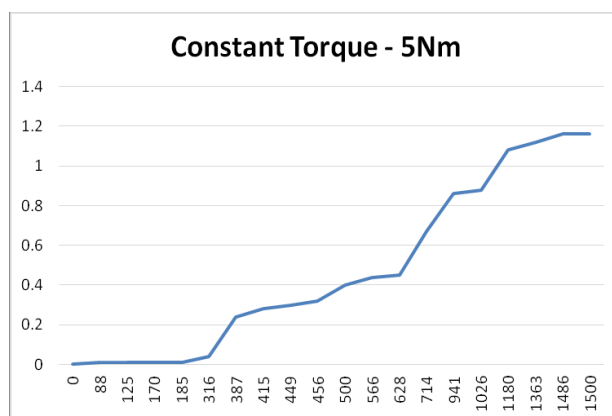
The Figure 3 presents the performance data acquisition from dynamo. Figure 3(a), 3(b) and 3(c) shows the brake power response to rpm at 2 Nm, 3 Nm and 5 Nm respectively. With increase speed, the brake power increases. At constant speed, the brake power is more for more torque application. The Figure 3(d) shows the noise level in decibel due to use of different blend of fuel.



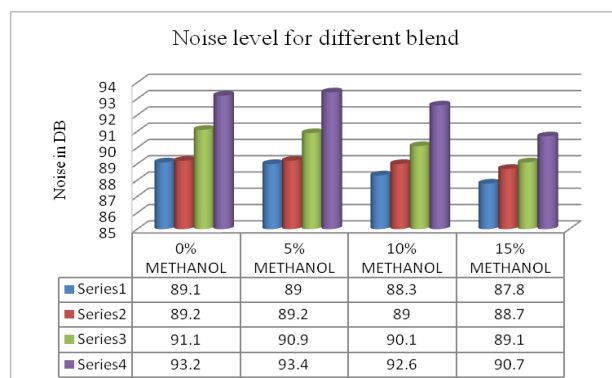
(a)



(b)



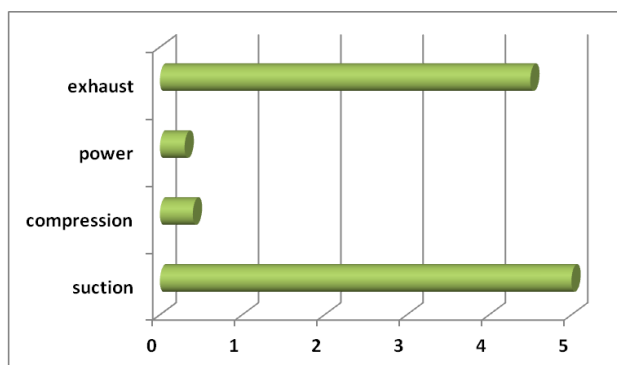
(c)



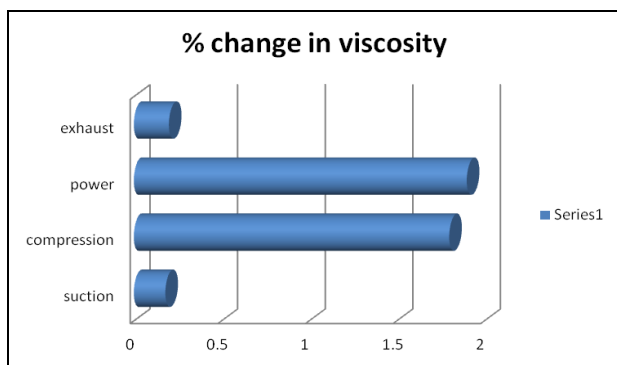
(d)

**Fig. 3.** Eddy current dynamometer measured performance output: (a) brake power response to 500 rpm, (b) brake power response to 1000 rpm, (c) brake power response to 1500 rpm and (d) Noise monitoring of different blend use.

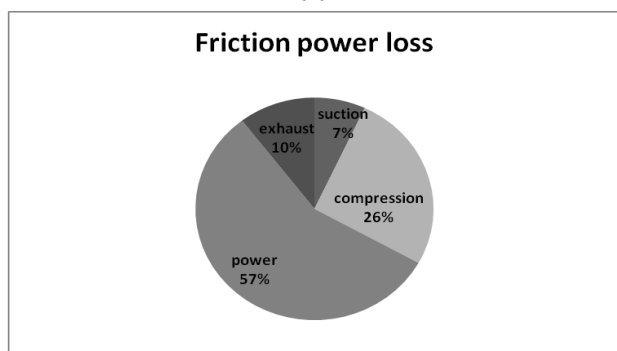
The Figure 4(a) shows the maximum value film thickness in different strokes. At suction and exhaust stroke, the film thickness is as high as 5  $\mu\text{m}$  and hydrodynamic situation prevails. While, during compression and power stroke because of dominance of gas pressure for enhanced sealing mode, the film thickness reduced to less than 0.5  $\mu\text{m}$ .



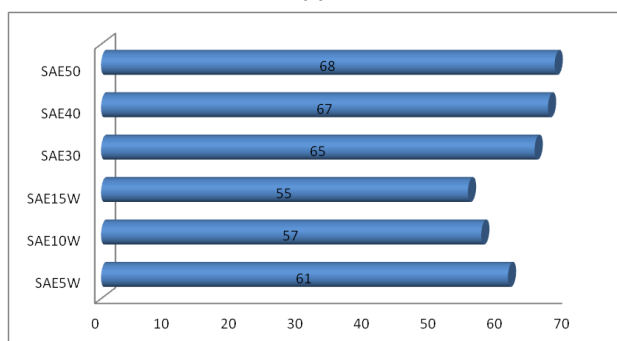
(a)



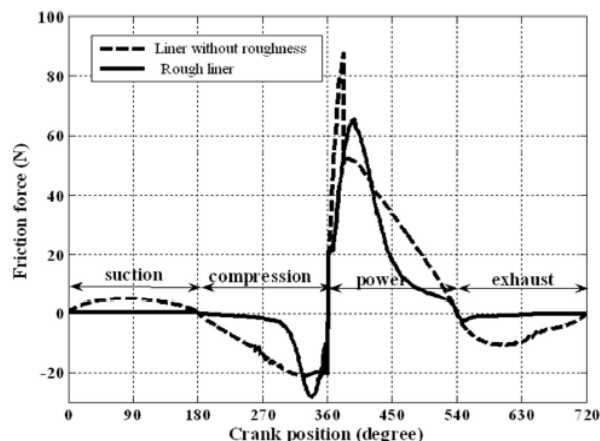
(b)



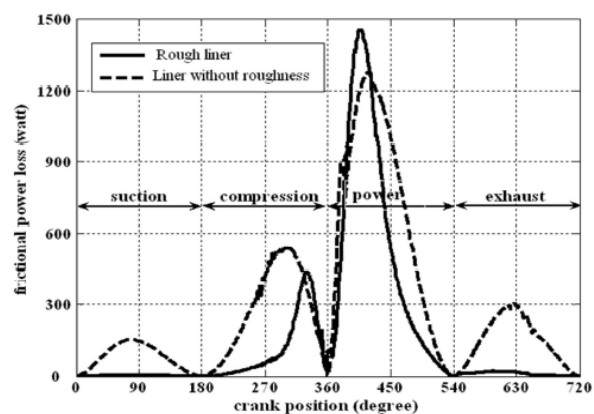
(c)



(d)



(e)



(f)

**Fig. 4.** Friction parameter monitoring: (a) Maximum film thickness for different stroke, (b) Maximum variation of viscosity ratio ( $\eta/\eta_0$ ), (c) Percentage of maximum power in different stroke, (d) Temperature variation due to oil grade change, (e) Cyclic friction force due to smooth and rough liner [11] and (f) Cyclic friction power due to smooth and rough liner [11].

Further, the Fig. 4(b) shows the viscosity ratio ( $\eta/\eta_0$ ) at different strokes. At compression and power stroke, it became 1.8 times due to increase in applied load on conjunction interface. The Fig. 4(c) shows that highest % of friction loss occurs in compression stroke (28 %) and power stroke (57 %). Further to this analysis, Fig. 4(d) represents the temperature rise for different lubricant grade. The Figures 4(e) and 4(f) show the effect of considering intentional rough surface on friction force and friction power. Roughing surface in a definite pattern, helps in reducing friction loss.

## 5. CONCLUSION

The paper discussed the condition monitoring of the ring considering emission and friction as

criteria for observation as bore that 47 % of energy is lost in these modes. The monitoring parameters are: Emission constituents of exhaust gas such as CO, CO<sub>2</sub>, NO<sub>x</sub>, HC, and O<sub>2</sub> are monitored at different speed and torque conditions. The analysis shows that use of blended fuel enhances the NO<sub>x</sub> level due to increasing in exhaust muffler temperature. The M15 blended fuel reduces the noise level. In friction monitoring the parameters helped in understanding the condition of the engine are film thickness, friction force, friction power and the oil viscosity. The compression and power stroke transition is more prone to energy loss, where more than 85 % of the energy loss occurs.

### Acknowledgement

We are very much thankful to the All India Council for Technical Education and Training (AICTE), New Delhi for funding this research. The funding of AICTE through RPS grant-in-aid to carry out our research project entitled “Advanced Engine Technology for Sustainable Development of Automotive Industry” is here acknowledged.

### REFERENCES

- [1] P.C. Mishra, *Modeling for friction of four stroke four cylinder petrol engine*, Tribology in Industry, vol. 35, no. 3, pp. 237-245, 2013.
- [2] N. Mittal, R.L. Athony, R. Bansal, C.R. Kumar, *Study of performance and emission characteristics of a partially coated LHR SI engine blended with n-butanol and gasoline*, Alexandria Engineering Journal, vol. 52, iss. 3, pp. 285-293, 2013, [doi: 10.1016/j.aej.2013.06.005](https://doi.org/10.1016/j.aej.2013.06.005)
- [3] P.C. Mishra, S. Kar, H. Mishra, A. Gupta, *Modeling for combined effect of muffler geometry modification and blended fuel use on exhaust performance of a four stroke engine: A Computational Fluid Dynamics approach*, Applied Thermal Engineering, vol. 108, pp. 1105-1118, 2016, [doi: 10.1016/j.applthermaleng.2016.08.009](https://doi.org/10.1016/j.applthermaleng.2016.08.009)
- [4] Y. Wang, L. Lin, A.P. Roskilly, S. Zeng, J. Huang, Y. He, X. Huang, H. Huang, H. Wei, S. Li, J. Yange, *An analytical study of applying Miller cycle to reduce NO<sub>x</sub> emission from petrol engine*, Applied Thermal Engineering, vol. 27, iss. 11-12, pp. 1779-1789, 2007, [doi: 10.1016/j.applthermaleng.2007.01.013](https://doi.org/10.1016/j.applthermaleng.2007.01.013)
- [5] A.A. Al-Farayedhi, A.M. Al-Dawood, P. Gandhidasan, *Effects of Blending MTBE with Unleaded Gasoline on Exhaust Emissions of SI Engine*, Journal of Energy Resources Technology, vol. 122, iss. 4, 239-247, 2000, [doi:10.1115/1.1288206](https://doi.org/10.1115/1.1288206)
- [6] X. Hua, C. Jiang, D.W. Herrinn, T.W. Wu, *Determination of transmission and insertion loss for multi-inlet mufflers using impedance matrix and superposition approaches with comparisons*, Journal of Sound and Vibration, vol. 333, iss. 22, pp. 5680-5692, 2014, [doi: 10.1016/j.jsv.2014.06.016](https://doi.org/10.1016/j.jsv.2014.06.016)
- [7] H.A. Moneib, M. Abdelaal, M.Y.E. Selim, O.A. Abdallah, *NO<sub>x</sub> emission control in SI engine by adding argon inert gas to intake mixture*, Energy Conversion and Management, vol. 50, iss. 11, pp. 2699-2708, 2009, [doi: 10.1016/j.enconman.2009.05.032](https://doi.org/10.1016/j.enconman.2009.05.032)
- [8] R.A. Baker Sr, R.C. Doerr, *Catalytic Reduction of Nitrogen Oxides in Automobile Exhaust*, Journal of the Air Pollution Control Association, vol. 14, no. 10, pp. 409-414, 1994, [doi: 10.1080/00022470.1964.10468305](https://doi.org/10.1080/00022470.1964.10468305)
- [9] X. Hua, Y. Zhang, D.W. Herrin, *The effect of conical adapters and choice of reference microphone when using the two-load method for measuring muffler transmission loss*, Applied Acoustics, vol. 93, pp. 75-87, 2015, [doi: 10.1016/j.apacoust.2015.01.014](https://doi.org/10.1016/j.apacoust.2015.01.014)
- [10] P.C. Mishra, *Tribodynamic modeling of piston compression ring and cylinder liner contact at high-pressure zone of engine cycle*, The International Journal of Advanced Manufacturing Technology, vol. 66, iss. 5-8, pp. 1075-1085, 2013, [doi: 10.1007/s00170-012-4390-y](https://doi.org/10.1007/s00170-012-4390-y)
- [11] P.C. Mishra, *A Review of Piston Compression Ring Tribology*, Tribology in industry, vol. 36, no. 3, pp. 269-280, 2014.
- [12] P.C. Mishra, H. Rahnejat, P.D. King, *Tribology of piston compression ring*, Woodhead publishing, Cambridge, UK, 2010.
- [13] P.C. Mishra, Prakhardeep, S. Bhattacharya, P. Pandey, *Finite Element Analysis for Coating Strength of Piston Compression in Contact with Cylinder Liner: A Tribodynamic Analysis*, Tribology in industry, vol. 37, no. 1, pp. 42-54, 2015.
- [14] H. Shahmohamadi, R. Rahmani, H. Rahnejat, C.P. Garner, P.D. King, *Thermo-Mixed Hydrodynamics of Piston Compression Ring Conjunction*, Tribology Letters, vol. 51, iss. 3, pp. 323-340, 2013, [doi: 10.1007/s11249-013-0163-5](https://doi.org/10.1007/s11249-013-0163-5)
- [15] P.C. Mishra, *Modeling the root causes of engine friction loss: Transient elastohydrodynamics of a*

piston subsystem and cylinder liner lubricated contact, Applied Mathematical Modeling, vol. 39, iss. 8, pp. 2234-2260, 2015, doi: [10.1016/j.apm.2014.10.011](https://doi.org/10.1016/j.apm.2014.10.011)

- [16] N. Patir, H.S. Cheng, *An Average Flow Model for Determining Effects of Three-Dimensional Roughness on Partial Hydrodynamic Lubrication*, Journal of Lubrication Technology, vol. 100, iss. 1, pp. 12-17, 1978, doi: [10.1115/1.3453103](https://doi.org/10.1115/1.3453103)
- [17] M. Loganathan, P. V. Manivannan, A. Ramesh, *Investigations on performance and emissions of a two-stroke SI engine fitted with a manifold injection system*, Indian Journal of Engineering and Material Sciences, vol. 13, no. 2, pp. 95-102, 2006.
- [18] S.S. Ragita, S.K. Mohapatra, K. Kundu, *Comparative study of engine performance and exhaust emission characteristics of a single cylinder 4-stroke CI engine operated on the esters of hemp oil and neem oil*, Indian Journal of Engineering and Materials Sciences, vol. 18, no. 3, pp. 204-210, 2011.
- [19] A. Jamrozik, W. Tutak, A. Kociszewski, M. Sosnowski, *Numerical simulation of two-stage combustion in SI engine with prechamber*, Applied Mathematical Modeling, vol. 37, iss. 5, pp. 2961-2982, 2013, doi: [10.1016/j.apm.2012.07.040](https://doi.org/10.1016/j.apm.2012.07.040)

$F_{2.5}(\lambda_{rk})$	Probability distribution of asperity height	
$F_{asp}$	Asperity contact pressure	$N$
$h_{sk}$ and $h_r$	Variable circumferential gap, Film thickness	$\mu m$
$K^*$	Constant used in calculation of asperity contact pressure	
$N_a$	Number of asperity per unit contact area	
$N$	RPM of the engine	$MPa$
$P_{asp}$	Asperity contact pressure	
$P_{mep}$	Mean effective pressure	$MPa$
$P_c(k)$	Power at $k^{th}$ crank angle	
$t$	Time	$sec$
$v$	Speed of entraining motion	$ms^{-1}$
$V_d(k)$	Displacement volume at $k^{th}$ crank angle.	
$x, y$	Co-ordinate directions	
$\eta$ & $\eta_0$	Lubricant dynamic viscosity and reference viscosity	$Pas$
$\rho$	Lubricant density	$kgm^{-3}$
$\tau$	Total Shear stress	$Nm^{-2}$
$\theta$	Crank location in degree	$m$
$\phi_p$	Pressure flow factor	
$\phi_s$	Shape flow factor	
$(\phi_{fg}, \phi_{fp}, \phi_{fs})$	Flow factors used for friction calculation	
$\beta_{rk}$	Asperity tip radius	$m$
$\mathcal{G}$	Damping factor	
$\left( \begin{matrix} \phi_p, \phi_s, \\ \phi_g, \phi_{fg}, \\ \phi_{fp}, \phi_{fs} \end{matrix} \right)$	Flow factors of geometry, pressure and shear	
$\lambda_{rk}$	Stribeck's oil film parameter	-

### Nomenclature

$A_i$ & $B_i$	Constant related to Fourier representation	
$B_v$	Parameter related gas blow by calculation	
$C$	Radial clearance	$m$
$D$	Diameter of the bore	$mm$
$E_c, E_r$	Young's modulus for cylinder liner and piston ring	$Nm^{-2}$
$E'$	Apparent modulus of elasticity of the contacting pair	$Nm^{-2}$
$F_f$	Fictional force due to hydrodynamic action	$N$